



Matching of Shapes Bound by Freeform Curves

M. Ramanathan

Indian Institute of Technology Madras, emry01@gmail.com

ABSTRACT

Matching and retrieval of shapes, both in two and three dimensions, have been a topic of interest to researchers in the field of computer graphics, vision and geometric modeling for at least a decade. In this paper, a shape is assumed to be represented as set of freeform curved boundaries. A prominent approach to matching curved outline is the graph-based approach, where a skeleton is used as a basis for obtaining the graph. In general, graph-matching is a hard problem and the comparison costs increase proportionally with graph size and hence slows down the process. In this paper, the skeleton, and in particular, medial axis of curved boundaries has been used. As opposed to using graph-based matching, statistical-based methods of signatures obtained from the properties of the skeleton have been employed. This enables a faster construction of shape signatures thereby increasing the speed of matching. Moreover, this facilitates the comparison of shapes that may have the presence of holes (inner loops) in it. In addition to the qualitative visualizations of retrieval results, retrieval performance by calculating quantitative statistics parameters typically used in shape matching is also discussed.

Keywords: shape matching, freeform curves, statistical approach, medial axis.

DOI: 10.3722/cadaps.2012.133-146

1 INTRODUCTION

Fundamental problems in shapes such as matching, retrieval, correspondence, segmentation, etc. have applications in computer graphics, computer vision, medical imaging, and biology among other fields. Among these problems, shape matching (essentially, a problem that finds similar shape to the query one) has gained particular importance as the technological advances in science (such as cryo-microscopy) and in engineering (e.g. laser scanned data) in recent years has resulted in a great explosion of data.

Approaches for shape matching include feature-based methods that use global properties such as moment invariants [11], Fourier descriptors [38, 33] and geometric ratios [36]. Histograms [1, 26] and shape distributions [34, 32] use properties such as distance, angle, area and volume between random points on the model. Lightfield descriptor (LFD) [7], a method that has been shown to give very good retrieval results, is a view-based method. LFD uses a collection of images from the model taken at the sampling points on a view sphere. The L_1 distance metric is then used as the similarity measurement.

Approaches in [22, 37] for matching have used the concepts from manifold learning. The central problem in machine learning is to “learn” a function based on a data set. The data set is assumed to be a sample from an unknown manifold. Approximations to the eigenvalues and eigenfunctions of the Laplace-Beltrami operator on this manifold were used to define eigenmaps [2] and an infinite collection

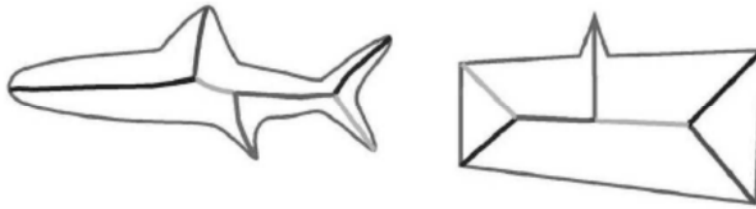


Fig. 1: Similar shock graphs for different objects [39].

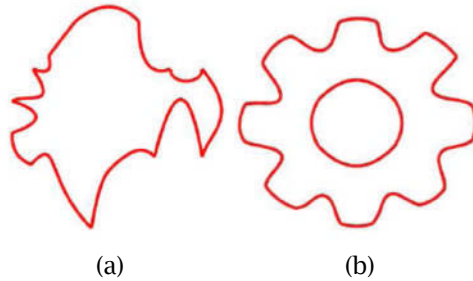


Fig. 2: Examples of shapes as used in this paper (a) a shape having only outer loop. (b) multiply-connected shape.

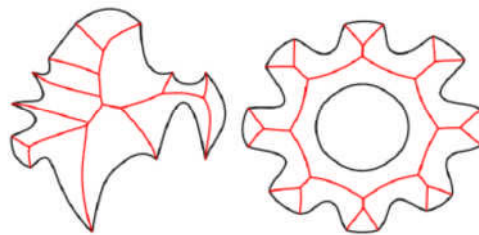


Fig. 3: Examples of MA.

of diffusion maps [9]. L´evy [28], draws an elegant analogy with Chladni plates and argues that the eigenfunctions of the Laplace-Beltrami differential operator understand the geometry, i.e., they capture the global properties of the surface. Rustamov [37] demonstrates their utility for deformation-invariant search using a global point signature (GPS). It is challenging to compute the eigenvalues and eigenvectors numerically, and approaches avoiding such explicit computation are desirable. The utility of these methods depend upon the quality of the descriptors which enter into the construction of the affinity matrices [22].

Local diameter, a statistical measure obtained using the neighborhood of a point, was used as a shape function in [16], which is called as diameter shape-function. Bending-invariant representation based on multidimensional scaling has been presented in [12]. This approach embeds (flattens) the computed geodesic distance into smaller dimensional Euclidean space, bringing all the models into a canonical pose. This method, though, has shown to be too sensitive to modifications and hard to control on general 3D meshes [16]. Research on partial shape matching using features has been the topic of [14, 15].

An object or a model or a shape in three dimensions can be represented either in a discrete form such as mesh, or in continuous form using Bezier/B-spline surfaces, termed as freeform surfaces. Correspondingly, in two dimensions, a discrete representation could be polylines and the continuous one by freeform curves. Most of the approaches discussed above have been applied to discrete representation. When the domain is represented as silhouettes obtained from images, prominent methods include skeletal context [48], contour-based descriptor [21, 27], graph-based approaches [39], Hausdorff distance [13], open curves [10], using uniformly chosen points [30], and shape geodesics [31]. When a freeform representation of the curve is used, metamorphosis has been employed in [8].

When a skeleton is computed for the outline, graph-based methods seem to be more prominent. This approach extracts structure from a model, by decomposing them into parts/components using skeletons. To compute them, models are either discretised using voxels [43, 44] or Voronoi and Delaunay complexes [24] are used. Sundar et al. [44] uses a skeletal graph as a shape descriptor to encode geometric and topological information. Shock graph along with edit distance was the approach used in [39]. Reeb graph [3, 19] is another approach to characterize the topology of the model. Graph-based methods are complex and susceptible to topology changes, in general. Moreover, graph-matching slows down as the comparison costs increase proportionally with graph size and is considered to be a hard problem. Also, at times, graphs need to be aligned [40]. It is also not sufficient to just use graph as they can be similar for different objects (Fig. 1) [39]. A detailed review of various shape descriptors for model retrieval can be found in [20, 45]. Various strategies that can be used when skeleton is employed can be found in [17].

In this paper, a shape is assumed to be defined by a set (not just a single closed curve) of non-self intersecting two-dimensional freeform C^1 -continuous curves connected together that form a closed loop. Adjacent curves intersect only at the common vertex at their ends (it is a *convex vertex* if the included angle is less than 180° or else it is termed as *reflex vertex*), and no two non-adjacent curves intersect (i.e. there is no intersection). However, they can form more than one loop - one outer loop and possibly several inner loops (shapes having inner loops are sometimes referred to as multiply-connected shapes). The shape is also assumed to be free of noise. It is believed that the richest shape variety can be reached by shapes or solids with free-form boundary curves/surfaces that are typically defined by Non-Uniform Rational B-Spline (NURBS) curves or surface patches [47]. Fig. 2 shows the example shapes used in this paper. The main contributions of this paper are

- As opposed to component-based or part-based approach typically used in skeleton-based shape matching which calls for identification of correspondences between shapes - a complex task by itself, in this paper, statistical-based skeleton property matching has been proposed and demonstrated.
- Footpoints, the corresponding points for a point on MA, appear to have been a neglected entity so far in matching, have been employed to define one of the shape functions.

2 SKELETON - MEDIAL AXIS TRANSFORM

The Medial Axis Transform was first introduced by Blum [4] to describe biological shape. It can be viewed as the locus of the center of a maximal disc as it rolls inside an object. Since its introduction, the MAT has found use in a wide variety of applications that primarily involve reasoning about geometry or shape. The Medial Axis(MA), or skeleton of the set D , denoted $M(D)$, is defined as the locus of points inside D which lie at the centers of all closed discs (or balls in three dimensions) which are maximal in D , together with the limit points of this locus. A closed disc (or ball) is said to be *maximal* in a subset D of the two dimensional (or three dimensional) space if it is contained in D but is not a proper subset of any other disc (or ball) contained in D . The radius function of the MA of D is a continuous, real-valued function defined on $M(D)$ whose value at each point on the MA is equal to the radius of the associated maximal disc or ball. The Medial Axis Transform (MAT) of D is the MA together with its associated radius function.

Properties of MA that aid immensely in shape matching are:

- Symmetry information: MA establishes an object centered representation from which individual shape characteristics can be measured.
- One to one correspondence: There exists a one to one correspondence between the object boundary and its MAT.
- Rigid-body transformation Invariance: As MA is a coordinate-system-independent abstraction, it is rotation, translation and uniform-scale invariant.
- Homotopy equivalence: A MA is homotopically equivalent to its object. This helps in identifying the homotopical characteristics of a shape such as the presence of holes in it.
- Shape function: Each point on the medial axis is associated with a radius function. This enables not only in the reconstruction of the shape but also can be used as a shape function that captures the local information. Moreover, other geometric properties such as curvature at a point on the medial axis can be computed and used as shape function.

Algorithm 1 ShapeMatching(shape)

```

for Each query/database shape do
  Compute MA using an algorithm (such as the one in [6]).
  Using the computed MA, obtain the shape function and then normalize.
  Compute the Histogram/Distribution.
end for
  Compute dissimilarity using a metric.

```

MA, in general, has the ability to capture the shape of the object very accurately. On the other hand, MA is susceptible to local changes in the shape - a small change in shape can cause significant topological changes in the MA. Moreover, a continuous description of the MA is possible from a continuous representation of the part only for the case of polygons where the boundary consists of linear segments or circular arcs [25]. For a part with non-linear or curved segments a continuous description of MA is only possible if the part representation is discretized/approximated using line segments, bi-arcs or point-set. It should be noted that, for objects with freeform boundaries, efficient and accurate computation of MA without discretising them is still a topic of interest for various researchers. However, this research, in the recent past, has revealed interesting algorithms and the MA can indeed be computed efficiently and accurately (see [6, 18]). Fig. 3 shows couple of examples of MA for shapes with freeform boundaries.

3 SHAPE MATCHING USING MA

A major challenge in the shape matching problem is to find a shape signature that can be constructed and compared quickly. Popular approaches such as graph-based ones are not efficient to handle [16]. The key idea is to use a local geometric derivative, MA, to obtain shape functions that can then be used to obtain shape signatures. Consider the radius function of MA. When the MA is used as a graph, across edges (simplified/MA segments [5]) of the graph, radius function can be defined. However, when a shape consists of boundaries represented as a set of freeform curves, capturing the changes accurately in properties such as radius function is not that easy. This is because, the radius function can be represented in closed-form only when a shape is composed of points, lines and circular arcs as MA is either linear or one of the conic sections [25]. This is not the case when arbitrary freeform curves are used as boundaries.

To compare shapes, a shape signature can be obtained either by using a histogram of the shape function or using a probability distribution function as in [34] rather than using closed-form representation of shape functions, which may not be available for freeform boundaries. Moreover, distribution-based approach avoids the need to compare graphs and graph-alignment and has shown to be very effective even for pose-oblivious shape search [16]. MA has the inherent capability to be a pose-invariant and can go even further to capture deformation-invariancy, at least up to isometry. The dissimilarity between objects is then evaluated using a metric such as L_N norm. The overall approach is illustrated in Algorithm 1.

3.1 Shape functions and signature from MA

The properties of the computed MA are used to define shape function. As MA is inherently attached to its corresponding footpoints, they are also been made use of (A point of contact with the domain boundary, of the underlying disk of a point on the MA is called the *footpoint* of the point on the MA).

- Distance between footpoints (DF);
- Radius function at a point on the MA (RF);
- Curvature at a point on the MA (CF);

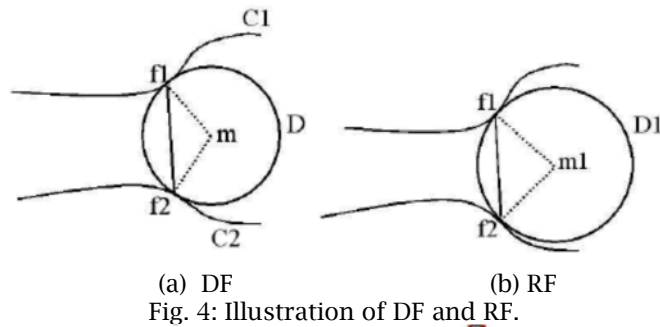


Fig. 4: Illustration of DF and RF.

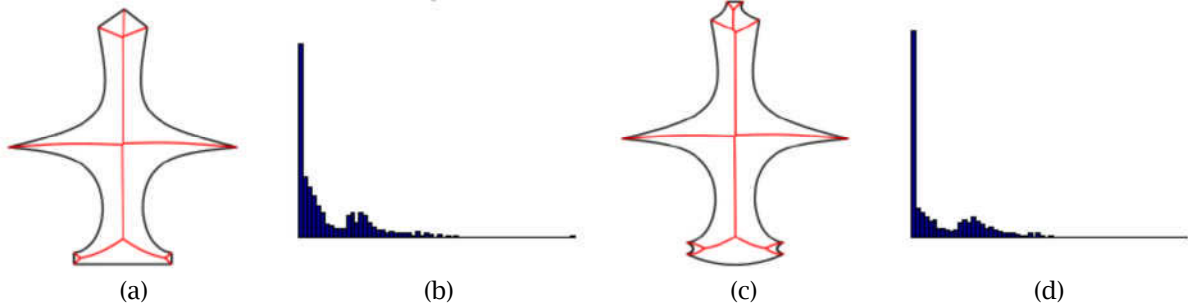


Fig. 5: MAT and signature from DF for two similar shapes.

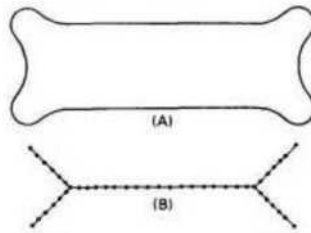


Fig. 6: Medial axis for a dog bone [5].

3.1.1 Obtaining shape signature

Initially, each function is computed for the points on the MA and the normalization is then done by dividing by the maximum value of the respective function. This process will yield the approximated probability value for each of the shape function, which can then be viewed as a histogram. The number of bins for generating the histogram is chosen as 64. These histograms are then used as shape signature of the respective shape function. Note that these functions are easy to compute once the MA is available and are invariant to rigid transformations. Uniform-scaling is alleviated by dividing with the maximum.

3.2 Distance between footpoints

MA provides an inherent correspondence between different points on the boundary curve as opposed to devising a separate approach for correspondence. Instead of measuring distance between two arbitrary points, in this approach, distance between the footpoints corresponding to a point on MA has been used. This is based on the premise that it approximates the local thickness of the shape. Fig. 4(a) shows the footpoints f_1 and f_2 corresponding to a point 'm' on the MA having the disc D . DF is the distance between footpoints f_1 and f_2 . Fig. 5 shows the MA and shape signature obtained using DF for two similar shapes. However, do note that the structure of the MA for the two shapes have variations (near the top end).

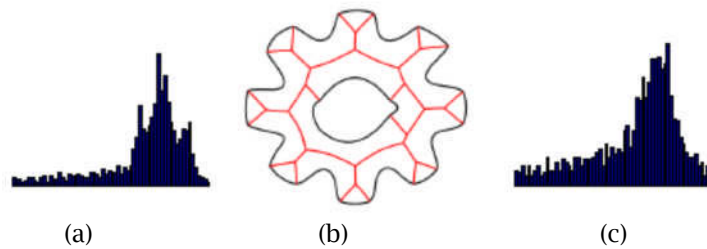


Fig. 7: (a) Signature from RF for Fig. 3(b); (b) and (c) MAT and its respective Signature from RF for a shape similar to Fig. 3(b).

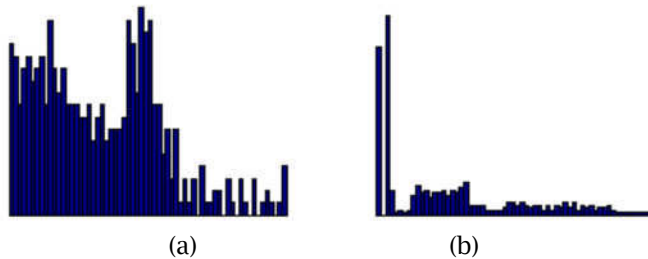


Fig. 8: Signatures from RF and CF respectively for MAT shown in Figure 5(a).

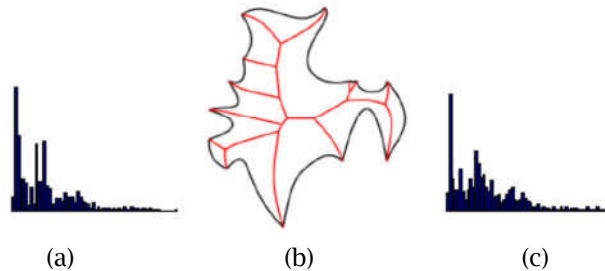


Fig. 9: Signatures obtained CF in (a) and (c) for shapes in Fig. 3(a) and Fig. 9(b) respectively.

3.3 Radius function

MA description is related to growing the shape boundaries in the direction orthogonal to the boundary as opposed to along the boundary. As MA can be considered to be placed in the center of the shape and also the union of maximal disks is the original shape itself, it is imperative to use the information from the disks. In particular, the radius of the maximal disks is used as a shape function and termed as RF. Radius function has the capability to distinguish shapes even when the medial axis can be same. A classic example to illustrate this is the dog bone (Fig. 6) whose medial axis is the same as that for a rectangle. However, the distinguishing feature there is the MAT, which includes the radius function and they are not the same for dog bone and rectangle. Figs. 7(a) and 7(c) show the shapes signatures from RF for similar shapes in Figs. 3(b) and 7(b) respectively.

Though this function appears to be similar to DF, it should be noted that radius can be different even when the distance between the footpoints are similar and vice versa. The disk D_1 in Figure 4(b) is different in radius when compared to D in Fig. 4(a) even though the footpoints f_1 and f_2 have the same distance in both of them. Hence the shape signatures derived from DF and RF is also different from each other. For the shape in Fig. 5(a), Fig. 5(b) shows the signature from DF, where as its signature from RF is shown in Fig. 8(a) and it is clear that they are distinct. Note that the radius at a convex vertex is zero and this has been included when computing the signature using RF.

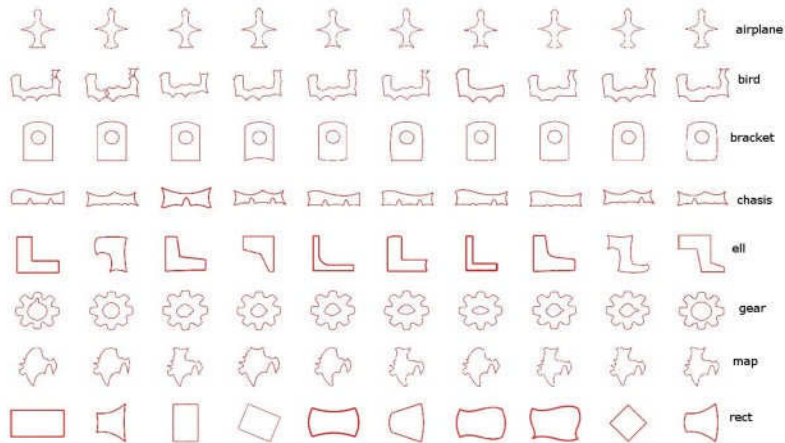


Fig. 10: Shapes in freeform database.

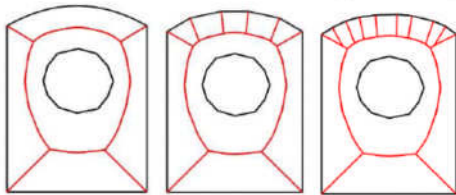


Fig. 11: MAT for similar shapes in the database.

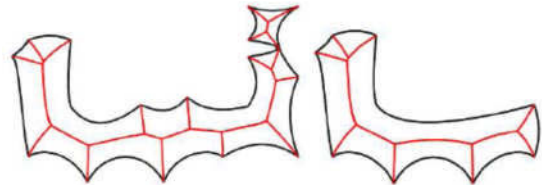


Fig. 12: Partially similar Shapes in freeform database.

3.4 Curvature at a point on MA

As the shape consists of freeform boundaries, the tangent and curvature at a point on the shape is well defined except at finite number of points (corners). Boundaries with zero curvatures (straight lines) are also considered. Curvature of the axis and the boundary has been effectively used to distinguish portions of a shape in [5]. In this paper, adjacent MA points are used to compute an approximate value for curvature. First, the tangent at a point on the MA is computed using the tangents at its footpoints. The magnitude of the change in tangents is used as curvature. It is then normalized for computing the shape signature which is then used for matching. Fig. 9 shows the signature obtained using the curvature function.

Though all the shape functions have been derived from MA, do note that they are also distinct. Figs. 5(b), 8(a), and 8(b) show the shape signature obtained using DF, RF and CF respectively for the shape in Fig. 5(a).

3.5 Similarity measurement

Given two shape signatures, its similarity can be computed using distance measures such as χ^2 , Minkowski's L_n , Mahalanobis etc. The shape signatures, in this paper are essentially one-dimensional vectors. Though may not be the best distance measure, for its simplicity, L_2 has been employed.

4 RESULTS AND DISCUSSION

4.1 Computing MA

As already noted, computation of MA for freeform objects have been of interest to researchers in the recent past. Recent developments indicate that quite a few algorithms for computing MA of freeform objects, at least in 2D can use the input shape without discretizing it. In this paper, the algorithm

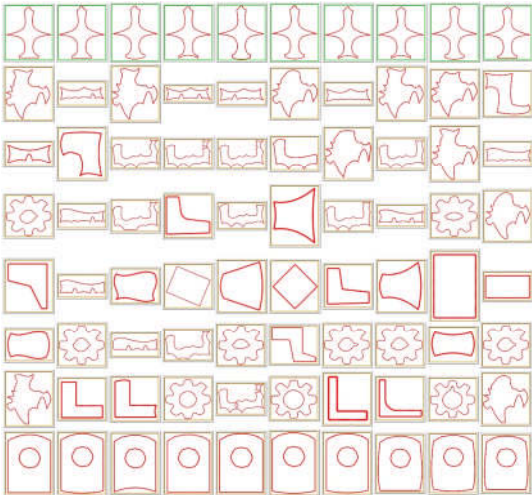


Fig. 13: All retrievals for the query input in the class 'airplane' of the shape function DF.

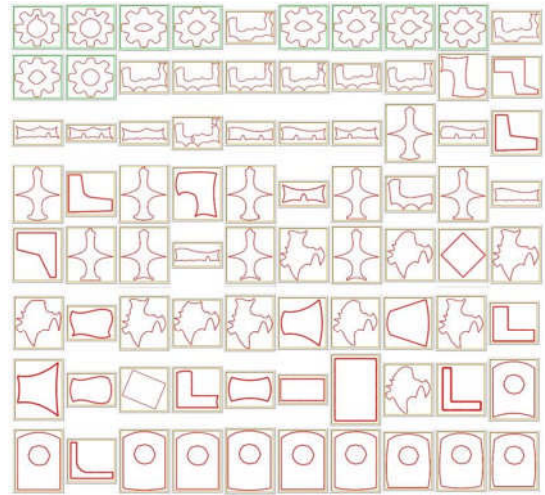


Fig. 14: All retrievals for the query input in the class 'gear' for the shape function RF.

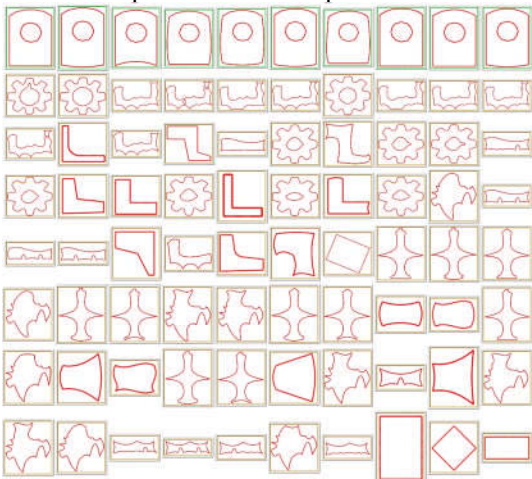


Fig. 15: All retrievals for the query input in the class 'bracket' for the shape function CF.

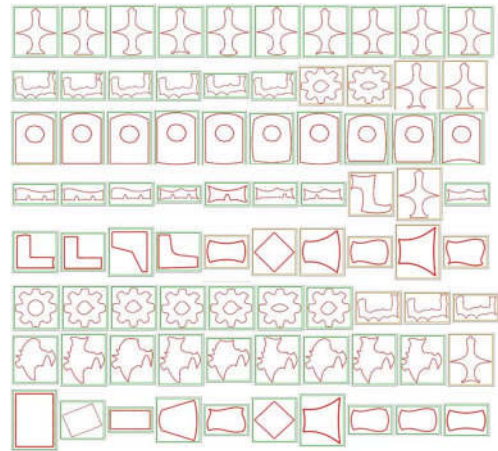


Fig. 16: First ten retrievals using DF signature for a shape in each class.

described in [35] has been used to compute MA, where the algorithm has the ability to computed for different step sizes on the 2D curved boundary (please refer to [35] for further details).

4.2 Database details

In this paper, a freeform database consisting of 80 shapes has been used to test the described approach. They have been classified as airplane, bird, bracket, chasis, ell, gear, map, and rect, as has been shown in the Fig. 10. Each one consists of 10 shapes that can be termed similar. To test the effectiveness of the proposed method, the database consists of many different traits. Within a class, shapes have holes as well as no-hole ones (see for example 'bird'). L-shaped (ell) objects consist of non-uniform scaled ones. Gear has varying shaped holes. The class 'Bracket' has a hole (inner loop) in all the shapes. The class 'rect' has shapes that are quite dissimilar but have the same structural arrangement of MA. They all distort either the MA structure or/and its properties. As an example, Fig. 11 illustrates one of the traits in the database - for similar shapes; number of MA segments is quite different from each other. The database also contains shapes that can be considered only partially similar (see Fig. 12). This database, essentially a manually constructed one, has been chosen not only to

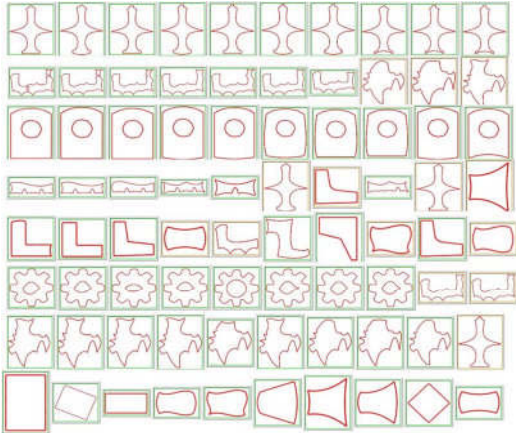


Fig. 17: First ten retrievals using RF signature for a shape in each class.

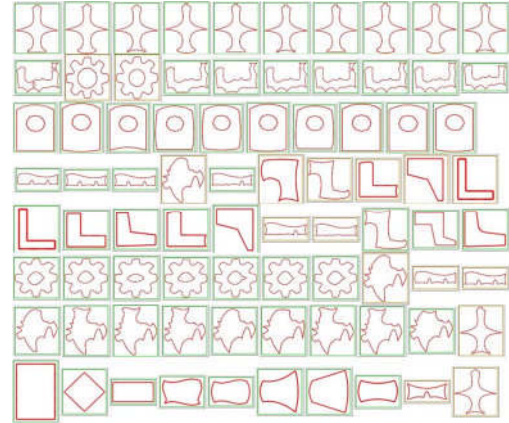


Fig. 18: First ten retrievals using CF signature for a shape in each class.

illustrate the strength of the approach presented in the paper, but also to indicate its possible shortfalls. It should be noted that the retrieval results of a matching algorithm is entirely dependent on the database set up that includes the definition of classes and shapes in each class.

4.3 Retrieval results - qualitative

Figs. 13 - 18 show the retrieval results qualitatively. In all the retrieval results, the first shape (in first row and first column) is the query shape and also it is the retrieved one. Figs. 13 - 15 show all the retrieved shapes for a shape in a class for the three shape functions respectively. Fig. 13 shows the retrieval for a shape in the 'airplane' class using signature from DF, where all the similar shapes are retrieved in the first row itself. Fig. 14 shows the retrieval for a 'gear' using signature from RF. Though not all similar shapes appear in the first row, some of them are retrieved in the second row. Figure 15 shows the retrieval for a multiply-connected bracket, where all the shapes in the same category are retrieved in the first row itself, in spite of the fact that some of them have different number of MA segments (Fig. 11) and hence considerably different MA structure. Figs. 16 - 18 show the first ten retrievals for a shape in each class. In all the classes and in all the shape functions (and their signatures), at least few of the shapes in the respective class were retrieved in the first row, indicating the effectiveness of the approach. Even for shapes with holes, the signatures retrieve their closer matches, as is evident from looking at the retrieved results.

4.4 Quantitative performance measurements

In addition to the qualitative visualizations of retrieval results, retrieval performance by calculating quantitative statistics parameters described in [42] are also evaluated. Specifically, mean first and second tier have been used. Rather than evaluating performance relative to a single query, the average performances over a set of 80 query shapes have been estimated.

4.4.1 First and second tier evaluation

First-tier and second-tier values are defined as percentage of models in the query's class that appear in top K matches, where K is dependent on the size of the query's class. The higher values of these statistics indicate better retrieval results.

Tables 1, 2 and 3 show the first and second tier percentage retrievals of each class for the shape functions DF, RF and CF respectively. Along with the qualitative results, the tables provide an insight into how the shape functions are performing. In all, the classes 'airplane', and 'bracket' have performed really well, both in first as well as in second tier, where the retrieval rate is 100% in the second tier. L-shaped (ell) class has shown rather not that good performance in DF and RF, where as it shows good improvements when CF is employed. This is because, the class 'ell' contains shapes that are of non-uniformly scaled ones, which affect the distance and radius functions, but not the curvature function

| Class | First tier (%) | Second tier (%) |
|----------|----------------|-----------------|
| airplane | 97 | 100 |
| bird | 47 | 59 |
| bracket | 86 | 92 |
| chassis | 57 | 62 |
| ell | 34 | 57 |
| gear | 44 | 66 |
| map | 87 | 92 |
| rect | 85 | 100 |

Tab. 1: First and second tier results for DF.

| Class | First tier (%) | Second tier (%) |
|----------|----------------|-----------------|
| airplane | 99 | 100 |
| bird | 49 | 62 |
| bracket | 92 | 95 |
| chassis | 49 | 62 |
| ell | 41 | 56 |
| gear | 73 | 58 |
| map | 91 | 91 |
| rect | 85 | 100 |

Tab. 2: First and second tier results for RF.

| Class | First tier (%) | Second tier (%) |
|----------|----------------|-----------------|
| airplane | 98 | 100 |
| bird | 70 | 81 |
| bracket | 97 | 99 |
| chassis | 29 | 43 |
| ell | 57 | 82 |
| gear | 56 | 74 |
| map | 77 | 82 |
| rect | 60 | 71 |

Tab. 3: First and second tier results for CF.

that much. The class 'rect' has performed well both in DF and RF but suffered in CF, the reason being it contains zero curvature as well as curved boundaries. The class 'bird' also suffers because it contains a shape with hole and also a shape that is only partially similar. However, the good point here is that, when the shape with hole is given as query, similar non-holed shape is also retrieved (see second row in Figs. 17 and 18) 'Map' has done well both in DF and RF compared to CF, as there are quite a few variations in the boundary curvatures of the shapes in the class. 'Gear' is also of similar case as that of 'map'. The holes in the gear vary in both size and shape creating larger variations in curvatures as opposed to the distance and radius functions. 'Chassis' has performed better in DF compared to RF and CF. This could be because the shapes in this class approximates the local thickness better, though a clear reason is not evident.

The strength of this method is, though at times the MA structure can vary significantly, similarities are captured. Moreover, it can handle shapes with holes (inner loops). However, the method is a more of global one and hence it cannot capture shapes that are only partially similar. Of course, the major assumption here is that the MAT can be computed accurately and efficiently for shapes with freeform boundaries without discretization. This could be considered as a major bottleneck, which is the case for many of the skeleton-based approaches.

4.5 Robustness

One factor that plays a very important role in the distribution-based approach is the sampling strategy. In this work, the sampling was done based on the length of each boundary and the approach is tested with increments of 0.01 (100 samples on a curve) initially. Though the sample size is maintained constant for all shapes, this induces variations in the number of points on the MA being used. The matching process does not appear to be disturbed too much by this variation as the retrieval results indicate. This, however, has to be tested in a larger database.

Retrieval effectiveness was also tested for 0.02 (200 sample points on a curve). The results appear to be fairly similar to the samples of 0.01. As an example, the first and second tier results for samples of 0.02 (for signature from RF) are given in Table 4, which is fairly similar to Table 2. Hence, the retrieval seems to be not dependant on the sample size. As long as the construction of MA is correctly performed, the results may not differ with respect to sample sizes, indicating the approach using MA along with distribution-based analysis is robust.

| Class | First tier (%) | Second tier (%) |
|----------|----------------|-----------------|
| airplane | 100 | 100 |
| bird | 49 | 64 |
| bracket | 91 | 95 |
| chassis | 44 | 54 |
| ell | 71 | 88 |
| gear | 56 | 74 |
| map | 91 | 91 |
| rect | 85 | 100 |

Tab. 4: Results for RF with sample size 0.02 for MAT.

| Computation of | Time (minutes) |
|--------------------------|----------------|
| MAT (sample size = 0.01) | 10 |
| Indexing and Retrieval | 2 |
| MAT (sample size = 0.02) | 6 |
| Indexing and Retrieval | 2 |

Tab. 5: Running time.

One of the very desirable properties of a shape signature is that it has one-one correspondence between a shape and its signature. It should be noted that MA as such may be same for two shapes, but MAT (MA with radius function here) will be unique and thereby signatures such as RF can be used to capture similarity. However, it may be difficult to prove that shape signature obtained using distribution is one-one, but the test results seems to be pointing to that (a case in point is [34], where it has been shown to be very effective). A test in a larger database will reveal further details.

4.1 Computation time

Running time for computation of MA and Retrieval has been shown in Tab. 5. The running time for computing MA took only 10 min. and for each shape function (such as DF), running time for indexing and retrieval was less than 2 minutes. The total computation (including all shape functions), the running time was less than 16 minutes, which is quite fast. This can be attributed to the simplicity of the distribution method for computing the signatures from the shape functions.

4.2 Comparison

Popular databases for shape search include the Princeton Shape Benchmark [42] for three dimensional computer graphics models, Engineering Shape Benchmark [23] for CAD models, Silhouette-database [41] for images etc. A look at the shape retrieval contest (SHREC) [46] homepage will reveal available databases in various categories. However, it appears that there is no database that caters to the needs of freeform curves. The closest ones seems to be [39, 41] and the MPEG-7 data set [31], which are actually an image database and hence converting them into freeform curves might require processing of the images, which could result in errors during the conversion. Moreover, the images do not seem to contain holes and even if they have, extracting them could be difficult.

As the closest ones seems to be [39, 41], which consists of 99 silhouettes represented as images, and 11 in each category and the MPEG-7 data set [31], we compare our approach against the inner-distance measure used in [29] and shape geodesics in [31] at a broad level. To compare, we only choose categories where the shapes are very similar within the respective categories, as shapes in each category of [39] don't appear to vary significantly (i.e. they are mostly articulated variations). For example, 'airplane' and 'bracket' have shapes that are very similar within the respective categories, whereas 'ell' has varied scaled shapes. The first and second tier results of the function DF, RF and CF are almost similar to the retrievals in [29] (see Table 4 in [29]), showing very high percentage. On the other hand, [29] requires shapes to be aligned for sampling and uses different parameters (such as sampling density etc.) for different databases. In our database, it should be noted that the shapes are not just articulated variants and still the retrieval performance is quite high. This paper shows that the MAT need not be restricted to articulated models and also avoid the exhaustive graph-based matching.

Ref [31] measures its retrieval performance using bull's eye test: for every image in the database, the top 40 most similar shapes are retrieved. At most 20 of the 40 retrieved shapes are correct hits. This appears to be the measure 'second-tier' used in our paper, where at times close to 100% retrieval has been achieved for categories where shapes are very similar within it. There are categories where the performance is poor, which can be attributed mainly due to large variations in the shape within that category.

4.3 Limitations

One of the major limitations of the proposed approach is that the shape signatures are global in nature and will not capture local changes. Hence, the signatures cannot be applied for partial matching of shapes.

4.4 Future work

Currently, the spatial distribution of the shape function has not been employed. Properties of MA such as homotopic equivalence were also not considered for this paper. As the strength of each shape functions vary, it is also imperative to find a suitable weighting scheme that can combine the advantage of each of them. Approaches such as visual saliency, described in [17] could be considered. The approach described in this paper has shown to work for multiply-connected objects, and hence it can be extended to CAD model search that often have the presence of holes, cavities, etc. This approach has also to be tested in a larger database.

5 CONCLUSION

In this paper, a statistical-based skeleton property matching has been proposed and demonstrated with respect to chosen shape functions for shapes bound by freeform curves. The shape functions have been derived from the MA of curved boundaries. It can also handle shapes with holes. This has the potential to replace component-based or part-based approach typically used in skeleton-based shape matching method.

6 ACKNOWLEDGEMENTS

I thank Indian Institute of Technology Madras for providing the support in conducting this research. I also thank all the reviewers for their valuable comments.

7 REFERENCES

- [1] Ankerst, M.; Kastenmueller, G.; Kriegel, H.-P.; Seidl, T.: 3d shape histograms for similarity search and classification in spatial databases. In *SSD '99: Proceedings of the 6th International Symposium on Advances in Spatial Databases*, London, UK, 1999. Springer-Verlag, pages 207-226.
- [2] Belkin, M.; Niyogi, P.: Laplacian eigenmaps for dimensionality reduction and data representation. *Neural Comput.*, 15(6), , 2003, 1373-1396, doi:10.1162/089976603321780317
- [3] Biasotti, S.; Giorgi, D.; Spagnuolo, M.; Falcidieno, B.: Reeb graphs for shape analysis and applications. *Theor. Comput. Sci.*, 392(1-3), 2008, 5-22. doi:10.1016/j.tcs.2007.10.018
- [4] Blum, H.: A transformation for extracting new descriptors of shape. *Models for the Perception of Speech and Visual Form*, 1967, pages 362-381.
- [5] Blum, H.; Nagel, R. N.: Shape description using weighted symmetric axis features, *Pattern Recognition*, 10, 1978, 167-180, doi:10.1016/0031-3203(78)90025-0
- [6] Cao, L.; Liu, J.: Computation of medial axis and offset curves of curved boundaries in planar domain. *Comput. Aided Des.*, 40(4), 2008, 465-475. doi:10.1016/j.cad.2008.01.002
- [7] Chen, D.-Y.; Ouhyoung, M.; Tian, X.-P.; Shen, Y.-T.; Ouhyoung, M.: On visual similarity based 3d model retrieval. In *Eurographics*, Granada, Spain, 2003, pages 223-232.
- [8] Cohen, S.; Elber, G.; Bar-Yehuda, R.: Matching of freeform curves, *Computer-Aided Design*, 29(5), 1997, 369-378, doi:10.1016/S0010-4485(96)00075-9
- [9] Coifman, R. R.; Lafon, S.; Lee, A. B.; Maggioni, M.; Nadler, B.; Warner, F.; Zucker, S. W.: Geometric diffusions as a tool for harmonic analysis and structure definition of data: Diffusion maps. *Proceedings of the National Academy of Sciences*, 102(21), May 2005, 7426-7431. doi:10.1073/pnas.0500334102
- [10] Cui, M.; Femiani, J.; Hu, J.; Wonka, P.; Razdan, A.: Curve matching for open 2d curves. *Pattern Recognition Letters*, 30(1), 2009, 1 - 10.

- [11] Cybenko, G.; Bhasin, A.; Cohen, K. D.: Pattern recognition of 3D CAD objects: Towards an electronic yellow pages of mechanical parts, *Smart Engineering Systems Design*, 1, 1997, 1-13.
- [12] Elad, A.; Kimmel, R.: On bending invariant signatures for surfaces, *IEEE Transactions on Pattern Analysis and Machine Intelligence*, 25(10), October 2003, 1285-1295. doi:10.1109/TPAMI.2003.1233902
- [13] Fudos, I.; Palios, L.: An efficient shape-based approach to image retrieval, *Pattern Recognition Letters*, 23(6), 2002, 731 - 741.
- [14] Funkhouser, T.; Shilane P.: Partial matching of 3d shapes with priority-driven search. In *SGP '06: Proceedings of the fourth Eurographics symposium on Geometry processing*, Aire-la-Ville, Switzerland, Switzerland, 2006. Eurographics Association, pages 131-142.
- [15] Gal, R.; Cohen-Or, D.: Salient geometric features for partial shape matching and similarity. *ACM Trans. Graph.*, 25(1), 2006, 130-150. doi:10.1145/1122501.1122507
- [16] Gal, R.; Shamir, A.; Cohen-Or, D.: Pose-oblivious shape signature, *IEEE Transactions on Visualization and Computer Graphics*, 13(2), Mar./Apr. 2007, 261-271. doi:10.1109/TVCG.2007.45
- [17] Goh, W.-B.: Strategies for shape matching using skeletons, *Comput. Vis. Image Underst.*, 110(3), 2008, 326-345. doi:10.1016/j.cviu.2007.09.013
- [18] Hanniel, I.; Muthuganapathy, R.; Elber, G.; Kim, M.-S.: Precise voronoi cell extraction of free-form rational planar closed curves. In *SPM '05: Proceedings of the 2005 ACM symposium on Solid and physical modeling*, New York, NY, USA, 2005. ACM, pages 51-59.
- [19] Hilaga, M.; Shinagawa, Y.; Kohmura, T.; Kunii, T. L.: Topology matching for fully automatic similarity estimation of 3d shapes. In *SIGGRAPH '01: Proceedings of the 28th annual conference on Computer graphics and interactive techniques*, New York, NY, USA, 2001. ACM, pages 203-212.
- [20] Iyer, N.; Jayanti, S.; Lou, K.; Kalyanaraman, Y.; Ramani, K.: Three-dimensional shape searching: state-of-the-art review and future trends, *Computer-Aided Design*, 37(5), 2005, 509-530. doi:10.1016/j.cad.2004.07.002
- [21] Jain, A.; Muthuganapathy, R.; Ramani, K.: Content-based image retrieval using shape and depth from an engineering database, In *International Symposium on Visual Computing (2)*, 2007, pages 255-264.
- [22] Jain, V.; Zhang, H.: A spectral approach to shape-based retrieval of articulated 3d models. *Comput. Aided Des.*, 39(5) 2007, 398-407. doi:10.1016/j.cad.2007.02.009
- [23] Jayanti, S.; Kalyanaraman, Y.; Iyer, N.; Ramani, K.: Developing an engineering shape benchmark for cad models, *Computer-Aided Design*, 38(9), 2006, 939-953. doi:10.1016/j.cad.2006.06.007
- [24] Joachim, T. D.; Giesen, J.; Goswami, S.: Shape segmentation and matching with flow discretization. In *Proc. Workshop on Algorithms and Data Structures*, 2003, pages 25-36.
- [25] Kim, D.-S.; Hwang, I.-K.; Park, B.-J.: Representing the voronoi diagram of a simple polygon using rational quadratic Bezier curves, *Computer-Aided Design*, 27(8), 1995, 605-614. doi:10.1016/0010-4485(95)99797-C
- [26] Kriegel, H.-P.; Kroeger, P.; Mashael, Z.; Pfeifle, M.; Pötker, M.; Seidl, T.: Effective similarity search on voxelized cad objects. In *DASFAA '03: Proceedings of the Eighth International Conference on Database Systems for Advanced Applications*, Washington, DC, USA, 2003. page 27.
- [27] Latecki, L. J.; Lakmper R.; Eckhardt U.: Shape descriptors for non-rigid shapes with a single closed contour. In *Proc. IEEE Conf. Computer Vision and Pattern Recognition*, 2000, pages 424-429.
- [28] Levy B.: Laplace-beltrami eigenfunctions towards an algorithm that "understands" geometry. In *SMI '06: Proceedings of the IEEE International Conference on Shape Modeling and Applications*, 2006, page 13, Washington, DC, USA, 2006, IEEE Computer Society.
- [29] Ling, H.; Jacobs, D. W.: Shape classification using the inner-distance, *IEEE Trans. Pattern Anal. Mach. Intell.*, 29, 2007, 286-299.
- [30] McNeill, G.; Vijayakumar, S.: 2d shape classification and retrieval. In *Proceedings of the 19th international joint conference on Artificial intelligence*, San Francisco, CA, USA, 2005. Morgan Kaufmann Publishers Inc, pages 1483-1488.
- [31] Nasreddine, K.; Benzinou, A.; Fablet, R.: Variational shape matching for shape classification and retrieval, *Pattern Recognition Letters*, 31(12), 2010, 1650 - 1657.

- [32] Ohbuchi, R.; Minamitani, T.; Takei, T.: Shape-similarity search of 3d models by using enhanced shape functions, In TPCG '03: Proceedings of the Theory and Practice of Computer Graphics 2003, page 97, Washington, DC, USA, 2003, IEEE Computer Society.
- [33] Ohbuchi, R.; Nakazawa, M.; Takei, T.: Retrieving 3d shapes based on their appearance. In MIR '03: Proceedings of the 5th ACM SIGMM international workshop on Multimedia information retrieval, New York, NY, USA, 2003. ACM, pages 39–45.
- [34] Osada, R.; Funkhouser, T.; Chazelle, B.; and Dobkin, D.: Shape distributions, *ACM Trans. Graph.*, 21(4), 2002, 807–832. doi:10.1145/571647.571648
- [35] Ramanathan, M.; Gurumoorthy, B.: Constructing medial axis transform of planar domains with curved boundaries, *Computer-Aided Design*, 35(7), June 2003, 619–632.
- [36] Rea, H. J.; Corney, J. R.; Clark, D. E. R.; Pritchard, J.; Breaks, M. L.; Macleod, R. A.: Part-sourcing in a Global Market, *Concurrent Engineering*, 10(4), 2002, 325–333, doi:10.1177/106329302129140214
- [37] Rustamov, R. M.: Laplace-beltrami eigenfunctions for deformation invariant shape representation. In SGP '07: Proceedings of the fifth Eurographics symposium on Geometry processing, Airela-Ville, Switzerland, Switzerland, 2007. Eurographics Association, pages 225–233.
- [38] Saupe, D.; Vranic D. V.: 3d model retrieval with spherical harmonics and moments, In Proceedings of the 23rd DAGM-Symposium on Pattern Recognition, London, UK, 2001. Springer-Verlag, pages 392–397.
- [39] Sebastian, T.; Klein, P.; Kimia, B.: Recognition of shapes by editing their shock graphs, *Pattern Analysis and Machine Intelligence*, IEEE Transactions on, 26(5), May 2004, 550–571.
- [40] Sebastian, T. B.; Klein, P. N.; Kimia, B. B.: Alignment-based recognition of shape outlines, In IWVF-4: Proceedings of the 4th International Workshop on Visual Form, London, UK, 2001. Springer-Verlag, pages 606–618.
- [41] Sharvit, D.; Chan, J.; Tek, H.; Kimia, B. B.: Symmetry-based indexing of image databases, *J. Visual Communication and Image Representation*, 9, 1998, 366–380. doi:10.1006/jvci.1998.0396
- [42] Shilane, P.; Min, P.; Kazhdan, M.; Funkhouser T.: The princeton shape benchmark, In Shape Modeling International, June 2004.
- [43] Siddiqi, K.; Shokoufandeh, A.; Dickinson, S. J.; Zucker, S. W.: Shock graphs and shape matching. In ICCV, 1998, pages 222–229.
- [44] Sundar, H.; Silver, D.; Gagvani, N.; Dickinson, S.: Skeleton based shape matching and retrieval. In SMI '03: Proceedings of the Shape Modeling International, 2003, page 290, Washington, DC, USA, 2003, IEEE Computer Society.
- [45] Tangelder, J.; Veltkamp, R.: A survey of content based 3D shape retrieval methods. In SMI '04: Proceedings of the Shape Modeling International, Washington, DC, USA, 2004, pages 145–156.
- [46] Veltkamp, R.: Shrec home page. <http://www.aimatshape.net/event/SHREC>, 2010.
- [47] Wolter, F. E.; Friese, K. I.: Local and global methods for analysis interrogation, reconstruction, modification and design of shape, In Proceedings of Computer Graphics International Conference, Geneva, Switzerland, 2000. ACM, pages 137–151.
- [48] Xie, J.; Heng, P.-A.; Shah, M.: Shape matching and modeling using skeletal context, *Pattern Recogn.*, 41(5), 2008, 1756–1767. doi:10.1016/j.patcog.2007.11.005